

Wind Tunnel Simulation of Changes in the Atmospheric Boundary Layer from Rural to Urban Terrain

D. C. STEVENSON and W. L. LEE

Mechanical Engineering Department, University of Canterbury, Christchurch.

ABSTRACT

A suburban area, Oakland, Christchurch, adjacent to open farmland was selected and modelled to the scale of 1:300.

Measurements of mean and fluctuating velocities, energy spectra and autocorrelation functions were taken with the wind tunnel running at a free stream speed of 17.6 m/sec. The mean velocity profile plotted exhibited an inner and outer logarithmic region. The height of the internal layer inferred from the intersection of the inner and outer logarithmic profiles and its growth rate were compared with theoretical predictions. The surface shear stress profile downstream from the terrain discontinuity was determined from the slope of the inner logarithmic profiles and was also compared with theories. From the longitudinal energy spectra and turbulence measurements, it was deduced that in the region near the change of terrain, the structure of the internal layer is largely independent of that in the undisturbed outer layer. Significant reduction of integral length scales was noticed in the internal layer immediately downstream of the terrain discontinuity.

INTRODUCTION

The response of a turbulent boundary layer to a sudden change in surface roughness has been the subject of a number of theoretical and experimental investigations. Many of the experimental investigations were carried out using artificial surface roughness in a geometric or uniform pattern.

An existing urban terrain was modelled in the University of Canterbury atmospheric boundary layer tunnel at a scale of 1:300. Fig.1 shows an aerial photograph of the actual urban terrain which has flat farmland to the NW, N and NE of the housing development. Prevailing winds in Christchurch are from the NE and strong NW Fohn type winds often occur from the NW direction.

This report describes wind tunnel tests and results for the wind blowing from the NE direction (Fig.2).

PREVIOUS WORK

Theoretical Work

Elliot (1958) first introduced the "internal boundary layer" concept when a turbulent layer encounters a sudden change of surface roughness. All velocity and shearing stress modifications due to the roughness transition take place below an interfacing surface which originates at the leading edge of the roughness (see Fig.3). Elliot assumed a new equilibrium profile and matched the horizontal velocity but permitted a shearing stress discontinuity at the interface.

Panofsky and Townsend (1964) modified Elliot's theory and avoided a shear stress discontinuity at the interface by assuming a velocity distribution to allow a continuous variation of shear stress from the surface of the internal boundary layer. They assumed a surface stress parameter S given by:

$$S = (U_{*1} - U_{*2})/U_{*1}$$

Their velocity distribution and that of Elliot are given in Fig.3.

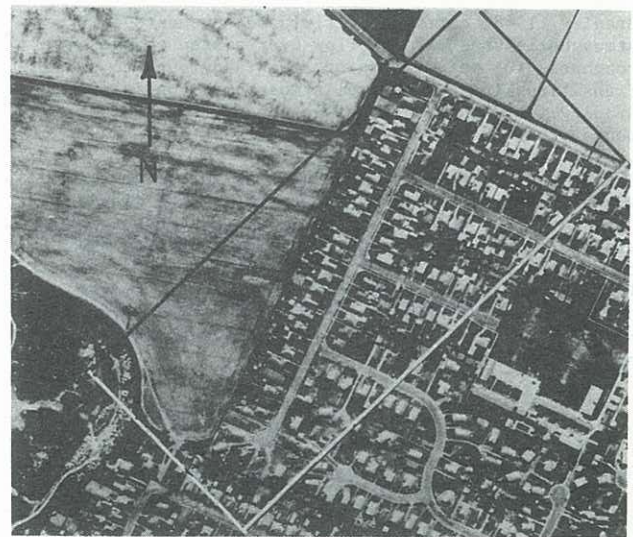


Fig.1: Aerial photograph of the suburb of Oakland. (The urban model is outlined.)

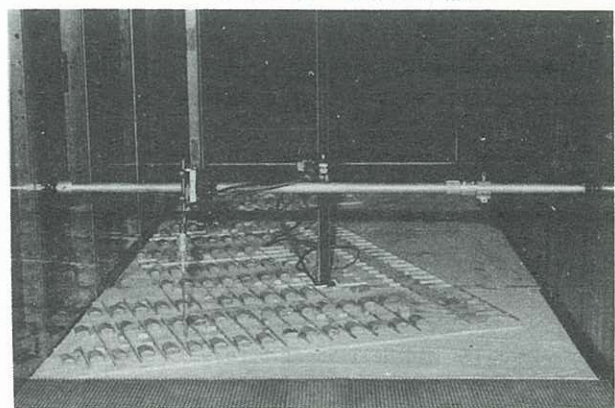


Fig.2: A view of the urban model in the wind tunnel (facing the south-west).

P.A. Taylor (1968) used the "mixing length" concept along with momentum and continuity to develop numerical methods for calculating changes over a surface roughness change. E.W. Peterson (1969) assumed the horizontal shear stress is proportional to the turbulent energy. Using numerical techniques he solved the momentum, continuity and turbulent energy

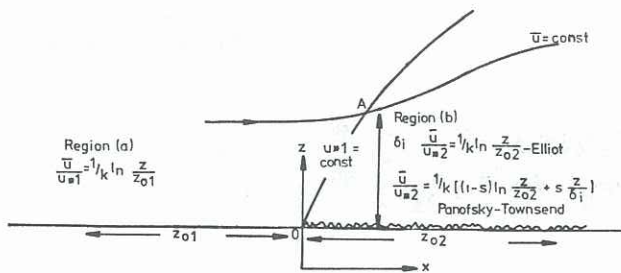


Fig.3: Schematic representation of the transition region smooth-rough flow.

equations assuming the flow is governed by the dominant terms.

Laboratory and Field Studies

Bradley (1968) carried out field measurements of atmospheric boundary low flow over a step change of roughness for both smooth to rough and rough to smooth transitions in near neutral atmospheric conditions. Bradley found that the surface shear stress adjustments occurred rapidly after the transition.

Antonia and Luxton (1971) used a low turbulence wind tunnel with rectangular slats normal to the flow and considered two cases; in the first the crests of the slats aligned with the upstream smooth surface and in the second the slats were upstanding from the surface. In both cases they found that the wall stress overshoots the equilibrium value after the transition and then returns more slowly to equilibrium as the flow proceeds downstream.

Panofsky and Peterson (1972) examined wind profiles over a change in terrain roughness from water to land for stable and unstable atmospheric conditions. Schofield (1977) collected a large array of data on the response of a turbulent flow change to surface roughness from smooth to rough and rough to smooth as well as flow with pressure gradients. He collated them in a coherent manner using parameters suggested by Townsend. He concluded that

$$\delta_i/z_{02} = 0.18(x/z_{02})^{0.92} \quad (1)$$

EXPERIMENTAL TECHNIQUES

Fig.2 shows the modelled site in the atmospheric boundary layer wind tunnel. A description of the wind tunnel and the properties of the simulated atmospheric boundary layer are given by Raine (1977). The T.S.I. hot wire probe is apparent in Fig.2. The probe output was coupled to a data acquisition system using a mini computer.

The flow, 0.4 m upstream of the roughness edge had a one-sixth power law profile and the upstream turbulence agreed with the ESDU profile.

RESULTS AND DISCUSSIONS

Velocity Profiles and Wall Shear Stress

The method used to determine the wall shear stress was applying the "law of the wall" for a rough surface given by the expression (Clauser 1956)

$$\bar{U}/U_* = (1/K) \ln(ZU_*/\nu) + c + \Delta\bar{U}/U_* \quad (2)$$

where $\Delta\bar{U}/U_*$ is a function of roughness $R.N.R_k = kU_*/\nu$

In general, for rough surfaces the vertical coordinate Z is measured from the "effective" origin of the rough surface. Experimental results have shown that this effective origin is at distance d above the wall where $d < k$ the height of the roughness elements. If the origin of Z is at the wall then in equation (2) Z is replaced by $(Z-d)$.

The value of d is found by trial and error by plotting the velocity profile using a logarithmic scale for Z , for different values of d . The plot that gives the best straight line profile gives the required value of d . The choice of the best line is not very sensitive to the value of d and this may account, in part, for the variation in d found in the literature. A value of $d = 3$ mm was found which gives $d/k = 0.26$ where k is the roughness height. Values of d/k in the literature vary from 0.18 to 0.40.

A plot of $(Z-d)$ and \bar{U}/\bar{U}_∞ is shown in Fig.4. From the slope of each graph the value of U_* and Z_0 can be obtained. Fig.4 shows that the velocity profiles change slowly with streamwise direction and that there is an overshoot at $x = 13.5$ cm. The velocity profiles in the upper region of the flow remain relatively constant indicating a region of undisturbed flow.

The non-dimensional variation of wall shear stress is plotted in Fig.5 where it can be seen that, following a sharp rise near the discontinuity, the wall shear stress then declines. The peak of the wall shear stress overshoot is approximately 20 roughness heights from the start of the discontinuity. Although the wall shear stress does not attain its equilibrium value immediately downstream of the roughness there is a rapid adjustment of the flow to a new value of shear stress. Also shown plotted in Fig.5 is the shear stress calculated using the relationship proposed by Clauser (1956). This shows the same trend but is a lesser value. The Clauser equation on Fig.5 is derived by matching the log law to a universal defect law for the outer layer that requires complete establishment of equilibrium across the whole boundary layer which is not fulfilled in this case. Peterson's theory predicts that only in the lower 10% of the internal layer is the flow in equilibrium with the new surface. It is considered that the wall shear stress obtained from the slope of the logarithmic velocity profile is more reliable in spite of the uncertainty in obtaining the value of d ; a larger value of d would give a corresponding smaller value of shear stress.

Similar trends on the value of τ_{02}/τ_{01} have been obtained by Bradley (1968) and Antonia and Luxton (1971) in spite of entirely different roughness elements.

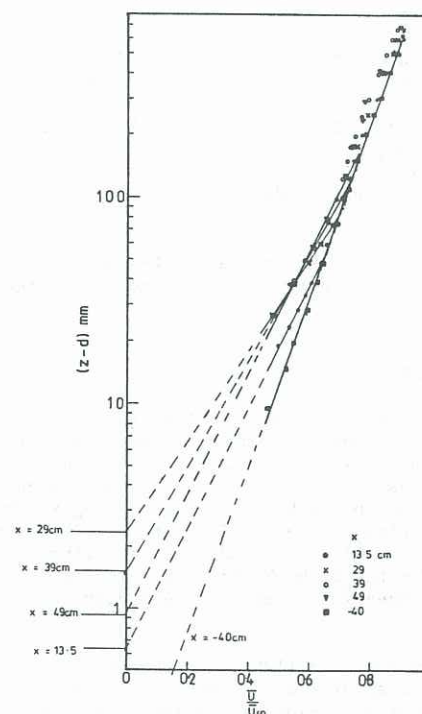


Fig.4: Determination of wall shear stress.

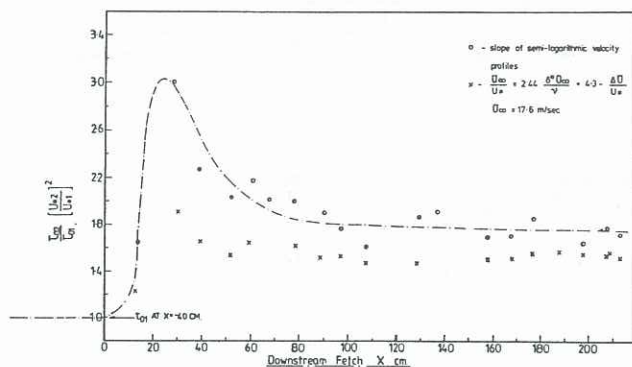


Fig.5: Wall shear stress distribution.

Fig.6 shows the comparison of the experimental wall shear stress parameters S (obtained from the slope of the semi-logarithmic profiles) with the theories of Panofsky-Townsend (1964) and Taylor (1968). Here the upstream roughness length (Z_{01}) was 0.18 mm and Z_{02} well downstream was 1.4 mm giving $M = \log(Z_{01}/Z_{02}) \approx -2$. With this value of M , predictions of both theories are shown in Fig.6.

Fig.6 also shows that for small values of x , there is a marked discrepancy when compared with both theories indicating that the theories do not apply for small x where rapid readjustment of the boundary layer is taking place.

The surface drag coefficient at the standard reference height of 10 m is defined as

$$k_{10} = (U_*/\bar{U}_{10})^2$$

For the scale of 1:300 the reference height is 0.33 mm and well downstream the velocity at this height is 7.9 m/sec. From Fig.5 the equilibrium value of U_*^2 is 1.36. This gives k_{10} as 0.022. This may be compared with the value of 0.20 - 0.045 quoted in the literature.

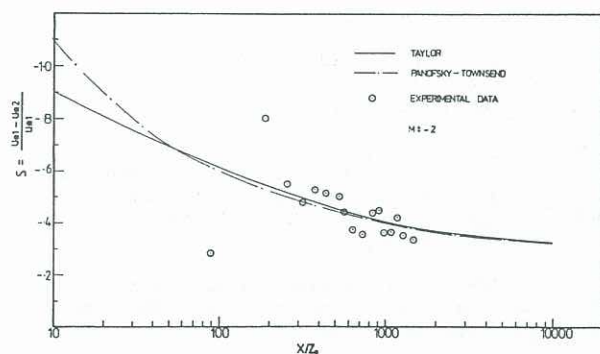


Fig.6: Distribution of surface stress parameter S .

Internal Boundary Layer

The depth of the internal boundary layer (δ_i) was obtained by means of the "merge" point. In Fig.7 the mean velocity profiles for successive positions downstream are plotted on a log-linear scale. The assumption of logarithmic profiles is reasonably well justified as most points fall on straight lines. The extent of the profiles increases with fetch indicating a return to equilibrium at large X . At $X = 10$ cm and 19.5 cm the velocity profiles show inflexion curvature. This is predicted in the theories of both Panofsky-Townsend (1964) and Peterson (1969) and also verified in experimental work by Bradley.

Fig.8 shows the growth of the internal boundary layer δ_i plotted in a non-dimensional form. Also shown are

theoretical predictions and experimental results for other workers. Except for the points at $X = 10$ cm and $X = 19.5$ cm, the results fit well into a curve defined by

$$\delta_i/Z_{02} = C(X/Z_{02})^n$$

with the value $C = 0.33$ and $n = 0.83$.

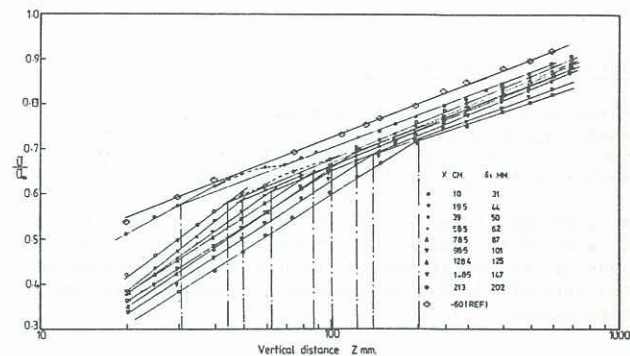


Fig.7: Internal boundary layer.

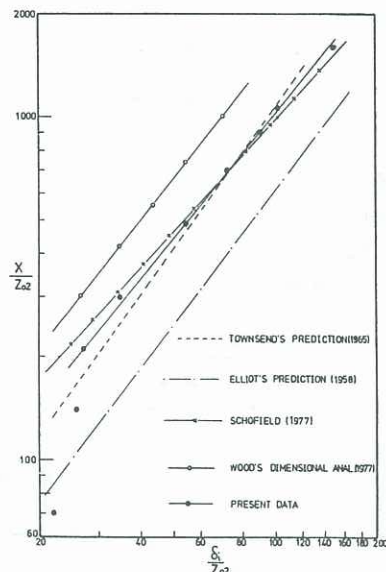


Fig.8: Growth of internal layer δ_i .

For large sets of experimental data Schofield (1977) found $C = 0.19$ and $n = 0.92$. Wood (1977) using dimensional analysis and experimental results found $C = 0.28$ and $n = 0.80$. Although the results for δ_i predicted by Elliot's theory are significantly higher than the present experimental results the power index n is in very good agreement with both Elliot's and Panofsky-Townsend's theories. The internal layer growth in this experiment can also be compared with the growth of a turbulent boundary layer on a flat plate ($\delta \sim X^{0.8}$).

Turbulence Intensity

Fig.9 shows the distribution of the local turbulence intensity with height Z . Shortly after the roughness increase ($X = 10$ cm) there is little difference in the turbulence intensity but as the flow proceeds downstream there is a sudden rise apparent at $X = 20$ cm. Not unexpectedly this is the same behaviour as shown for the wall shear stress (Fig.5). For $Z < 20$ mm the points are within the roughness elements and cannot be taken as an indication of a general trend in the profile.

Energy Spectra

Longitudinal energy spectra were obtained at four streamwise distances for four heights at each distance. Some general trends were observed.

1. As the flow moved into the internal layer there was a sudden jump in the high frequency energy.
2. As the wall was approached in the internal layer then the high frequency energy increased.
3. As the wall was approached in the internal layer the low frequency decreased.

Autocorrelation Coefficients

These were obtained for the same locations as the energy spectra and along with the energy spectra were used to estimate the longitudinal integral length scales of turbulence which are given in Table 1.

As expected, there is some discrepancy in these values because of the difficulty of estimating either the peak of the energy spectra or due to fluctuations in the autocorrelation coefficients, especially at long time delays.

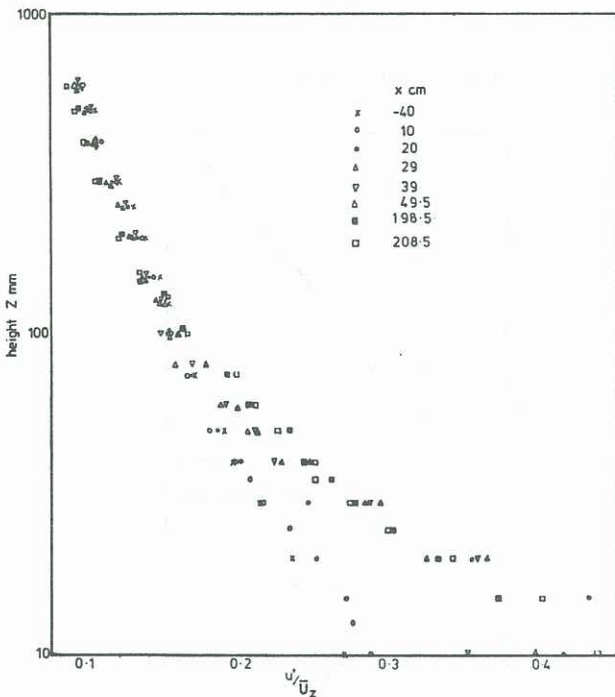


Fig.9: Variation of local turbulence intensity.

REFERENCES

Antonia R A; Luxton R E (1971): The response of a turbulent boundary layer to a step change in surface roughness. *J. Fluid Mech.*, 48, 721-761

Streamwise Location	Height z mm	n_p	Longitudinal Integral Length Scale L_{ux} cm	
			Derived from Spectra $L_{ux} = \frac{0.146 \times \bar{u}}{n_p}$	Derived from Autocorrelation $L_{ux} = \bar{u} \times T_E$
$x = 0$	50	4.5	39	30
$x = 10$ cm $\delta_i = 31$ mm	20	8.8	8.2	9.9
	30	4.6	18.9	18.6
	40	3.7	24.5	27.2
	80	4.3	23.9	25.3
$x = 58.5$ cm $\delta_i = 62$ mm	50	6.5	12.4	15.1
	70	5.8	14.7	19.1
	90	3.8	23.7	21.8
	150	4.9	19.6	30.2
$x = 78.5$ cm $\delta_i = 87$ mm	50	4.7	16.5	16.3
	70	3.1	27.1	18.02
	90	3.0	29.3	25.3
	150	4.6	20.8	23.3
$x = 200$ cm $\delta_i = 180$ mm	70	2.8	12.7	21.2
	150	4.4	22.0	24.9
	175	6.2	16.0	28.3
	250	4.7	22.1	29.8

Table 1: Tabulated longitudinal length scale data.

Bradley E F (1968): A micrometeorological study of velocity profiles and surface drag in the region modified by a change in surface roughness. *Quart. Journal of Royal Met. Society*, 94, 361-379.

Clauser, F H (1956): The turbulent boundary layer. *Advances in Applied Mechanics*, vol.IV.

Elliot W P (1958): The growth of the atmospheric internal boundary layer. *Trans. Amer. Geophys. Union*, 39, 1048-1054.

Panofsky H A; Peterson E L (1972): Wind profiles and change of terrain roughness at Risø. *Quart. Jnl Roy. Met. Soc.*, 98, 845-854.

Panofsky H A; Townsend A A (1964): Change of terrain roughness and the wind profile. *Quart. Jnl Roy. Met. Soc.*, 90, 147-155.

Peterson E W (1969): Modification of mean flow and turbulent energy by a change in surface roughness under conditions of neutral stability. *Quart. Jnl Roy. Met Soc.*, 90, 147-155.

Raine J K; Stevenson D C (1977): Wind protection by model fences in a simulated atmospheric boundary layer. *J. Ind. Aero.*, 2, 159-180.

Schofield W H (1977): The response of turbulent shear flows to discontinuous changes in surface roughness. *ARL-Mech.-Eng-Report-150*, Defence Science and Technology Organisation, Aeronautical Research Laboratories, Melbourne, Australia.

Taylor P A (1969): On the wind and shear stress profiles above a change in surface roughness. *Quart. J. Roy. Met. Soc.*, 95, 77-91.

Wood D H (1977): The growth of the internal layer following a step change in surface roughness. *I.C.Aero TN 77-101*, Imperial College of Science and Technology, Department of Aeronautics, London.